

Long-term power degradation analysis of crystalline silicon PV modules using indoor and outdoor measurement techniques

Fabian Carigiet^{a,b,*}, Christoph J. Brabec^{b,c}, Franz P. Baumgartner^a

^a Institute of Energy Systems and Fluid Engineering, School of Engineering, ZHAW Zurich University of Applied Sciences, Technikumstrasse 9, 8401, Winterthur, Switzerland

^b Institute Materials for Electronics and Energy Technology, FAU Friedrich-Alexander University Erlangen-Nürnberg, Martensstraße 7, 91058, Erlangen, Germany

^c Helmholtz Institute Erlangen-Nürnberg Forschungszentrum Jülich, Im Neuenheimer Feld 2, 91058, Erlangen, Germany

ARTICLE INFO

Keywords

c-Si solar cell
Outdoor test field
Solar simulator measurement
Outdoor performance monitoring
Performance ratio
Degradation rate

ABSTRACT

Annual degradation rates of PV modules are important in the yield prediction. For a high-quality PV module, these rates are lower than the measurement uncertainty of a nominal power measurement performed in today's most advanced certified photovoltaic reference laboratory. Therefore, the analysis requires a well thought out methodology that can compare the data relative to each other or relative to an unused module stored in the dark on an annual base. Over the past 10 years, several multi-c-Si and HIT modules have been accurately monitored in a string and single module setup by an outdoor performance measurement system. Additionally, all modules have been dismantled and measured using an indoor flasher measurement system once every year. With this unique measurement setup, the annual degradation rates of multi-c-Si modules and HIT modules are quantified based on three different analysis methodologies. The multi-c-Si modules showed an average annual degradation rate of $0.18\% \pm 0.06\%$ and $0.29\% \pm 0.06\%$ measured by the outdoor and indoor system, respectively. The indoor analysis of the HIT modules yielded an average annual degradation of $0.26\% \pm 0.06\%$. That corresponds to half of the degradation observed by the outdoor analysis method. Further evaluations of the performance ratio PR confirmed the results gained by the indoor methodology. The comparison of the standard PR with a temperature-corrected PR_{STC} for both technologies showed that the benefit of the lower temperature coefficient of the HIT technology is eliminated by its worse low light behaviour.

1. Introduction

One of today's most challenging parameters in the field of photovoltaic are the long-term degradation rates of PV modules and their uncertainties. It is the key for the economic calculation of the PV power plant yield over its service life. Reducing the uncertainties of the long-term yield predictions directly reduce the plant price due to the reduction of the economic risks. Performance loss rate (PLR) is a widely used indicator to specify the PV power plant performance over time. PLR is a complex interaction of the degradation of PV module nominal power, individual soiling, increasing ohmic losses in the PV plant wiring due to degradation of the electrical interconnectors and inverter efficiency drift related to semiconductor degradation. To achieve accurate and reliable results on PV plant PLR, a lot of manpower, time and effort must be spent on the proper monitoring of different PV systems using high-quality

measurement setups. The key to a successful PLR analysis is to separate the different loss mechanisms such as the usually predominating degradation of the PV module nominal power. This effort needs investment in high-quality sensor and metering equipment together with manpower over many years to achieve accurate and reliable results. It will not be achieved by the development of a quick data mining approach because it depends on the quality of the measurement data and not the amount.

Various literature [1–4] from different laboratories include degradation rates for different PV module technologies using their individual analysis technique with either indoor or outdoor data. The compendium of photovoltaic degradation rates [4] includes degradation rates from different PV module technologies and climates collected from various international studies. For c-Si PV modules that are monitored periodically over multiple years in moderate climates since 2010, the median degradation rate is lower than 0.5%. The compendium also shows that

* Corresponding author. Institute of Energy Systems and Fluid Engineering, School of Engineering, ZHAW Zurich University of Applied Sciences, Technikumstrasse 9, 8401, Winterthur, Switzerland.

E-mail address: fabian.carigiet@zhaw.ch (F. Carigiet).

<https://doi.org/10.1016/j.rser.2021.111005>

Received 10 June 2020; Received in revised form 23 February 2021; Accepted 18 March 2021

Available online 29 March 2021

1364-0321/© 2021 The Authors. Published by Elsevier Ltd. This is an open access article under the CC BY license (<http://creativecommons.org/licenses/by/4.0/>).

List of abbreviations

| | |
|-------------------|---|
| oSi | Crystalline silicon |
| DUT | Device under test |
| FF | Fill factor |
| HIT | Heterojunction with intrinsic thin layer |
| HJT | Heterojunction technology |
| MPP | Maximum power point |
| OC | Open circuit |
| PLR | Performance loss rate |
| POA | Plane of array |
| PR | Performance ratio |
| PR _{STC} | Performance ratio corrected at T _{STC} |
| PV | Photovoltaic |
| SC | Short circuit |
| SVFB | Swiss mobile flasher bus |
| STC | Standard test condition |
| TC | Temperature coefficient |

there are very few studies for HIT PV modules where the PV modules were monitored periodically since 2010. However, the median of the HIT degradation rates was shown to be around 1% for non-continuously monitored PV modules over all climates.

The presented results were established by a detailed analysis of highly accurate indoor and outdoor measurements of crystalline silicon

PV modules over 9 years [54]. All modules have been installed and monitored on a rooftop in Dietikon, Switzerland, since 2009 (Fig 1a). Once a year, the modules were dismantled (Fig 1b) and measured indoor by the Swiss Mobile Flasher Bus (Fig 1c) equipped with a high-quality industrial flasher. The two completely different measurement setups and analysis methods are used to identify the degradation rates for multi oSi and HIT modules under outdoor conditions. Furthermore, the unique outdoor measurement setup allows gaining information about the losses in the cabling by comparing the measurements of the single and the string application. Finally, the presented fitting method of the outdoor data is also used to analyse the temperature coefficients of each analysed year. This is done for the single module as well as the string application and for the operating points at open circuit and MPP.

2. Measurement setup and equipment

The unique outdoor PV test power plant was designed in collaboration between ZHAW and the electric utility EKZ and was installed at the technical headquarters of EKZ in Dietikon, Zurich in December 2009. The installation contains multi-crystalline silicon (multi oSi, Sunways) and high efficiency mono-crystalline heterojunction silicon (HIT, Sanyo). Table 1 contains the detailed data of the two different PV module types and their string configurations, which are analysed in this work.

The module mounting position and electrical wiring was not changed during the whole period of monitoring. Not one of these analysed multi oSi and HIT modules had to be replaced, providing a very good base for

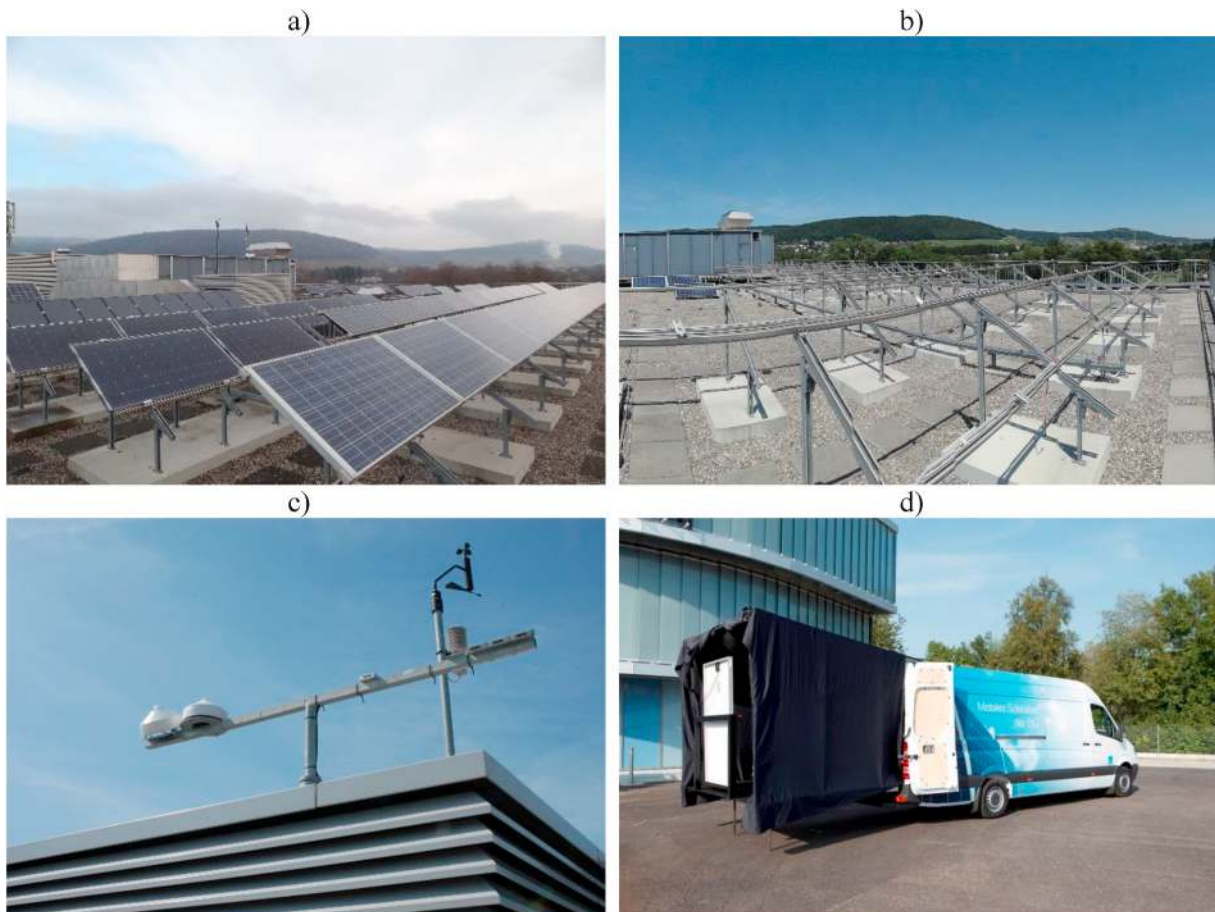


Fig. 1. The outdoor PV test plant is equipped with 66 modules of different PV module technologies shown in the photo a). All modules were dismantled once a year as can be seen in the photo b) to be measured indoor with the SVFB in photo c) [7]. The PV test power plant is equipped with a weather station including pyranometers and silicon reference cells shown in photo c).

Table 1
Since 2009, different PV module technologies were monitored at the same time [5]. In this work, the focus lies on the multi oSi and HIT module technology. The shown parameters represent datasheet values and string configurations

| General information and string configuration | | | Module parameter | | |
|--|------------|-------------|-------------------------|---------|-------|
| Manufacturer | Sunways | Sanyo | Manufacturer | Sunways | Sanyo |
| Model | SVR21QJA65 | HIP-215NK-E | Nominal power P_N [W] | 230 | 215 |
| Technology | multi oSi | oSi/aSi HIT | V_{MPP} at STC [V] | 29.3 | 42.0 |
| Module efficiency | 13.8% | 17.1% | I_{MPP} at STC [A] | 7.86 | 5.13 |
| Installation date | Sep 2009 | Sep 2009 | V_{OC} at STC [V] | 36.9 | 51.6 |
| Total # modules | 15 | 10 | I_{SC} at STC [A] | 8.34 | 5.61 |
| Nominal power P_N [W] | 3450 | 2150 | $TC P_{MPP}$ [%/K] | -0.43 | -0.30 |
| Tilt angle [°] | 30 | 30 | $TC V_{OC}$ [%/K] | -0.36 | -0.25 |
| Mounting # serial modules | Fix 15 | Fix 10 | $TC I_{SC}$ [%/K] | 0.06 | 0.03 |
| # parallel branches | 1 | 1 | Length [m] | 1.68 | 1.58 |
| V_{MPP} at STC [V] | 439.5 | 420 | Width [m] | 0.99 | 0.798 |
| I_{MPP} at STC [A] | 7.86 | 5.13 | Area [m ²] | 1.663 | 1.261 |
| V_{OC} at STC [V] | 553.5 | 516.0 | # serial cells | 60 | 72 |
| I_{SC} at STC [A] | 8.34 | 5.61 | Tilt angle [°] | 30 | 30 |
| | | | Weight [kg] | 24 | 15 |

analysing the degradation rates

2.1. Indoor monitoring (Swiss Mobile Flasher Bus)

The Swiss Mobile Flasher Bus (SMFB) was developed in 2009 with the aim of bringing the PV test laboratory to the customer's site by needing only a standard driver's license. Therefore, a large Mercedes-Benz Sprinter Panel Van has been equipped with a commercial high-quality PASAN sun simulator 3c. The main characteristics are [7]:

- 10ms pulsed light source
- Class AAAA
- Irradiated surface of 2m x 2m
- 5.5m light tunnel with 5 diaphragms for light trapping
- Optical filters set for low light and spectral response measurements

A platform can be pulled out of the backside of the SMFB, on which a scaffold can be mounted. This structure is covered with a black cloth used in photographic labs to build the dark 5.5m light tunnel with 5 diaphragms for light trapping. The device under test (DUT) is placed at the end of the tunnel and the xenon lamp, the capacitor bank, the electronic load and the control hardware are installed behind the driver's cabin. Additionally, different optical filters can be moved in front of the light source to measure the low light performance and the spectral response respectively. The irradiance on the DUT can be adjusted by using 4 different optical filters (100W/m², 200W/m², 400W/m² and 700W/m²). For the spectral response measurement, optical bandpass filters (15 filters at 50nm each) are used ranging from 400nm to 1100nm [8].

The maximum area of the DUT is 2m by 2m. The non-uniformity of the irradiance within this area is better than 1% (class A). This criterion together with the stability criteria of the irradiance during the pulse (<1%) and the quality criteria of the spectrum being also class A results in an overall class AAAA measurement system [7].

The maximum pulse duration of the light source is 10ms. During that time interval, the electronic load measures the I-V characteristic at a maximum sample rate of 40% within an adjustable electrical range of 300V/30A [7]. For PV modules with a high capacitance e.g. HIT PV modules, a longer light pulse duration would be needed. Therefore, a multi-flash mode is available, whereby the IV curve is split in parts and measured separately. The number of light pulses can be adjusted for each high capacitive PV module technology individually.

A detailed uncertainty budget was estimated, resulting in an overall measurement uncertainty of 3.2% (k = 2) [8]. In 2011, an intercomparison was performed between the SMFB and the stationary EU JRC ESTI calibration lab resulting in a maximal difference of nominal power measurement of less than 0.5% for the same DUT (oSi Module) [9]. Five years later, an additional round robin test confirmed that result and underlined the stability of the SMFB [10]. Fig. 1d shows the SMFB in operation.

2.2. Outdoor monitoring of the PV test power plant

The outdoor test field consists of a string and a single reference module for each technology. The reference modules are not connected to the string but mounted in between the string modules. The string is feeding the electricity into the grid via standard inverters available on the market. The voltage and current of the DC and AC side of the inverter is measured and logged. Simultaneously, the I-V curves of the single reference modules are measured by the electronic loads with four-terminal sensing. Between the I-V scans, the module is tracked at MPP. All these reference modules are equipped with one PT100 temperature sensor that is attached on the PV module backside. Several meteorological sensors are installed to measure the irradiances, ambient temperature, wind speed and direction. The setup includes six irradiance sensors – two for the global horizontal irradiance (pyranometer Kipp&Zonen GMP21 and non-filtered monocrystalline silicon ISE reference cell) and four for the plane of array (POA) irradiance (pyranometer Kipp&Zonen GMP21, non-filtered and filtered monocrystalline silicon ISE reference cells). All these irradiance sensors were recalibrated once in 2015. The outdoor test field and the meteorological equipment is shown in Fig. 1c.

Each sensor is logged every 2s and the mean minute value is stored in the database. Additionally, a second value per sensor is stored in the database that is synchronised with the start of the I-V curve measurements carried out once per minute. The following Table 2 shows all parameters of the outdoor measurement system including intervals and uncertainties.

A log file is in place to track the occurring measurement or system errors, the software updates, the changes in the test setup, the irradiance sensor cleaning and the people that are visiting or working on the roof.

Table 2
Measurement intervals and uncertainties of the indoor and outdoor setup. The uncertainties are relative to STC values except for the module temperature (70 °C).

| Measurement | Interval | | Uncertainty (k = 2) | |
|---------------------------|-------------------|---------------------|---------------------|-------|
| | minute mean value | minute single value | multi o-Si | HIT |
| Irradiance (pyranometer) | X | x | 1.19% | |
| Module temperature | x | x | 0.58% | |
| DC voltage (String) | x | x | 0.14% | 0.33% |
| DC power (String) | x | x | 0.19% | 0.36% |
| DC voltage (Module) | | x | 0.24% | 0.20% |
| DC power (Module) | | x | 1.24% | 1.32% |
| PR _{bc} (String) | x | x | 1.21% | 1.24% |
| PR _{bc} (Module) | | x | 1.72% | 1.78% |
| Flasher measurement | | | 3.20% | |

The records include when, by whom and why there was interference with the measuring system. As a result, each affected sensor is marked for the specified time interval within the analysis tool and excluded from the analysis.

2.3 Framework conditions

The outdoor monitoring started on 1st of March in 2010. In the first two years, a lot of knowledge about the operation of the monitoring system was gained and optimised, such as temperature sensor mounting, irradiance sensor cleaning, maintenance service of the automatic data acquisition system and analysis of the electrical data sets. This knowledge is the key for analysing the degradation rates because the presented and applied methods are very sensitive to these types of measurement and the resulting annual degradation rates are usually lower than 1%. The experience led to a proper sensor mounting using heat-conducting paste and capton tape since September 2010. This type of mounting is renewed every year after the fasher session. Furthermore, the sporadic irradiance sensor cleaning was changed to monthly based cleanings since June 2012. The verification of the test setup including the influence of the sensor cleaning is shown in Fig 2 as an example of the temperature coefficient (TC) analysis performed by a linear regression between PV module power and temperature at MPP. The plot shows a downward drift of the linear relationship between power and temperature at MPP. The reason for that is that the sensor cleaning was not frequent enough. For the plot b), the pyranometer was used for the data selection. This type of irradiance sensor shows a lower sensitivity to soiling because of its spherical dome. Since June 2012, the sensors have been cleaned on a monthly basis.

3 Analysis methodology

Three different analysis methodologies are applied to analyse the degradation rates. First, the degradation rates of the indoor STC power measurements are carried out. Then, the linear fitting of specifically selected outdoor data close to STC irradiance and the calculation of the annual PR over 10 years of outdoor operation enable the determination of two further degradation rates.

The uncertainties related to the determined degradation rates will be given directly in the results section together with the value in the form $\pm \sigma$ ($k = 1$). The measurement uncertainties and uncertainties of the calculated performance ratios are given in Table 2. Finally, the uncertainties of the annual STC power determined by the linear regression are lower than 0.59% (single module) and 0.61% (string modules) for

the multi-c-Si PV modules and $k = 1$. The corresponding uncertainties of the HIT modules are lower than 0.71% (single module) and 1.06% (string module).

3.1 Indoor methodology

The PV modules from the reference PV power plant were dismantled for the indoor characterisation each year until 2017. After that, the procedure has been changed to a two-year interval. The measurement procedure took place in spring or summer. Before each measurement session, the modules were cleaned and stored in the same room where the measurement took place, so that the module temperatures were stabilised and close to the ambient room temperatures. The temperature was measured on the backside of each module by a PT100 sensor and the temperature correction to 25°C STC condition was performed using the typical PV module manufacturer temperature coefficients.

The duration to complete the indoor measurement procedures was between three to four days in each year. Therefore, the stability and reliability of the measurement system was verified by measuring a calibrated multi-c-Si PV reference module (Sunways SIM210 UA65) before each measurement session and after each measurement interruption. These measurements were also used to recalibrate the measurement system. The calibration factor was within $\pm 1.1\%$ during all those measurement campaigns and showed no long-term trend. The reference module has been stored in dark over all the years since commissioning of the SIMFB in 2009.

There are two different I-V curve measurement modes used. The multi-c-Si modules are measured directly (from I_{SC} to V_{OC}) within a single 10 ms light pulse by the SIMFB (Fig 1d). Conversely, the HIT modules need a longer light pulse due to the higher capacitive junction. Therefore, the measurement of the I-V characteristic is split into 15 direct measurements with light pulse duration of 8 ms each. The 250 and 600 data points are stored in a database together with the extracted parameters such as I_{SC} , I_{MPP} , V_{OC} , V_{MPP} , P_{MPP} , FF, R_S and R_P .

The degradation rate is calculated by the linear regression of all P_{MPP} indoor measurements between 2011 and 2019. The first two years are disregarded to avoid the influence of initial degradation of c-Si PV modules on the long-term degradation rates. This is done for the single reference module and the average module power of the string.

3.2 Outdoor methodology

The analyses focus on STC power and voltage parameters for a single module and a string application on a yearly basis. The irradiance related

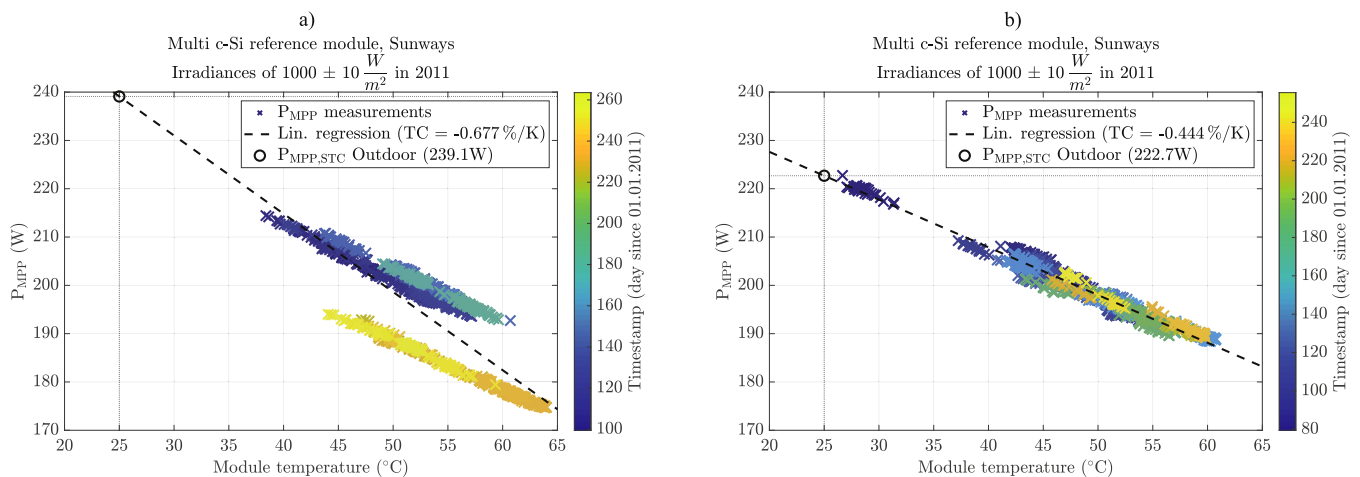


Fig 2. The two graphics include the P_{MPP} measurements of the multi-c-Si module at STC irradiance ($1000 \pm 10 \text{ W/m}^2$) with respect to its temperature in 2011. The colouring indicates the day of the year starting at the 1st of January. The data selection for plot a) was done based on the non-filtered monocrystalline silicon ISE reference while in plot b) the pyranometer was used.

evaluations and the selection of the data in the first step are performed using the pyranometer data oriented in plane of array. Additionally, only the data were processed on which clear sky condition prevailed to reduce transient effects of the sensors and DUT. The clear sky detection is performed by the algorithm developed at the Sandia Labs, US [11]. This model uses five parameter differences between the modelled clear sky and the measured irradiance data. The whole irradiance dataset is divided into 10min intervals for which the clear sky model is compared to the measurement according to the five criteria in Table 3. The measured irradiance is classified as clear sky if all five criteria are fulfilled. This classification is performed for each interval.

The voltage, power and temperature measurements in 1-min intervals are then selected according to these clear sky days in each year providing that the irradiance was within $1000 \pm 10 \text{ W/m}^2$. The linear correlation between the determining PV parameters and the module temperatures is used to extract the STC value by linear regression method as shown in Fig. 2b) for the MPP power or Fig. 9 for the MPP and open circuit voltage of both module technologies in 2012. The module temperatures are measured only at the backside of the single reference modules. Therefore, the assumption was made that the string modules have the same temperatures. This procedure is repeated for each year. Finally, the degradation rate is extracted in the same way as for the indoor analysis using the linear fit of all P_{MPP} measurements between 2011 and 2019. Again, this was done for the single reference module as well as for the string.

The second method calculates the annual PR and the annual temperature-corrected performance ratio PR_{STC} at T_{STC} according to the standard IEC 61724-1 (2017). This is done for the single module and the string including all measurements and not only clear sky measurements as in the previous explained method. Every mentioned PR value is determined on the DC level and regarding STC power from the datasheet unless otherwise mentioned. This method is needed as an additional verification and it can be used to explain some differences between indoor and outdoor analysis or single module and string analysis.

The entire analysis is performed using the POA pyranometer measurements because these sensors are less sensitive to soiling and they showed less long-term degradation than the crystalline reference cells, even though they were recalibrated 5 years after commissioning. As mentioned before, the pyranometer measurement are used to determine the clear sky condition and select the data (power, voltage and module temperature) for the irradiance condition $1000 \pm 10 \text{ W/m}^2$. A linear regression is performed between the selected power and module temperature to determine the power at STC as seen in Fig. 2b). There is an angular and spectral mismatch between the DUT and the pyranometer. The evaluation of the angle of incidence for the described data selection for the year 2011 showed that the average angle of incidence was around 11° . Thus, it can be assumed that angular mismatch is close to 1. The spectral mismatch is assumed to be small and constant during noon throughout the analysis. This yields to a small and constant error in the absolute value of the fitted annual STC that is consistent across all fitted STC values and should not affect the slope of the final regression for the determination of the degradation rate. Furthermore, Fig. 3b) illustrates the spectral mismatch at irradiance levels of around 800 W/m^2 . The analysis performed by a secondary class pyranometer leads to an intraday drift of the power or current vs temperature behaviour that is

caused by the spectral mismatch between the pyranometer technology and the c-Si module technology. The influence of the spectral mismatch can be reduced either by performing the analyses around 1000 W/m^2 or by using a crystalline ISE reference cell as shown in Fig. 3a). For the sake of completeness, the voltage vs temperature is not affected by this mismatch.

4 Degradation results of multi c-Si and HIT modules

The long-term degradation is calculated by a linear regression of P_{MPP} values over the time in years gained from the indoor and outdoor methodology. The indoor measurement from 2009/10 and the outdoor measurement from 2010 are excluded to select between the initial PV module degradation and the long-term degradation processes.

The manufacturers of the analysed PV module technologies guarantee an annual degradation of 0.8% (multi c-Si Sunways) and 1.0% (HIT Sanyo), respectively. Nowadays, the guaranteed annual degradation rates for the both PV module technologies are in the range of 0.5% [12,13].

4.1. Multi c-Si modules from sunways

The analysis of the indoor measurements of the multi c-Si modules in Fig. 4 shows an annual degradation of $0.23\% \pm 0.12\%$ for the single reference module and an average degradation of $0.29\% \pm 0.08\%$ for the string. The outdoor methodology yields slower annual degradation rates of $0.19\% \pm 0.07\%$ and $0.18\% \pm 0.08\%$, respectively. Ignoring the initial degradation and looking at the total degradation during 8 years of operation, the absolute degradation difference (average of reference and string modules) between the indoor and outdoor results is 0.6% and very small. This is very promising for the used methods which deal not with the absolute STC uncertainty but only the relative change of the nominal PV module power close to STC conditions. This determined degradation value is much smaller than the absolute measurement uncertainty of a single PV module STC measurement performed in today's most advanced certified photovoltaic reference laboratory. It must be considered that the PV modules were cleaned before the indoor measurements took place, which is a difference in the DUT setting of the comparison.

The gained results are less than or equal to the median of the degradation rates for c-Si PV modules installed in the last decade according to the study compendium of photovoltaic degradation rates.

For c-Si PV modules that are monitored periodically over multiple years in moderate climates since 2010, the median degradation rate is around 0.3% [4].

4.2. HIT modules from sanyo

The analysis of the indoor measurements of the HIT modules in Fig. 5 shows similar results to the multi c-Si modules. The annual degradation is $0.29\% \pm 0.08\%$ for the single reference module is close to the $0.26\% \pm 0.08\%$ representing the average value for the string. The outdoor analysis yields annual degradation rates that are twice as high ($0.53\% \pm 0.08\%$ for the single reference module and $0.50\% \pm 0.08\%$ for the string modules).

The further analysis based on the PR evaluation in Fig. 6 supports the achieved indoor results for the single ($0.29\% \pm 0.07\%$) and the string modules ($0.28\% \pm 0.08\%$). The most obvious explanation for these losses is an increased series resistance originating in the cabling system because it appears only at high irradiance in the STC fitting method. The two module types have different connectors (Tyco for Sunways and MC3 for Sanyo modules). The comparison of the outdoor measurements between the multi c-Si modules and the HIT modules resulted in a 3.3 times higher voltage drop in the string cabling. The single module is measured by four-terminal sensing but that is after the first connector. Therefore, the connection points are the most obvious source of the losses that are not eliminated by the measurement setup.

Table 3
Five criteria and their applied thresholds for the clear sky detection.

| Criteria | Threshold values |
|------------------------|--------------------------------|
| Mean value difference | $\pm 100 \text{ W/m}^2$ |
| Max value difference | $\pm 100 \text{ W/m}^2$ |
| Length difference | $-5 < L < 10$ |
| Variance of slope | $0 < \sigma < 0.05 \text{ Hz}$ |
| Max deviation of slope | $\pm 12 \text{ W/m}^2$ |

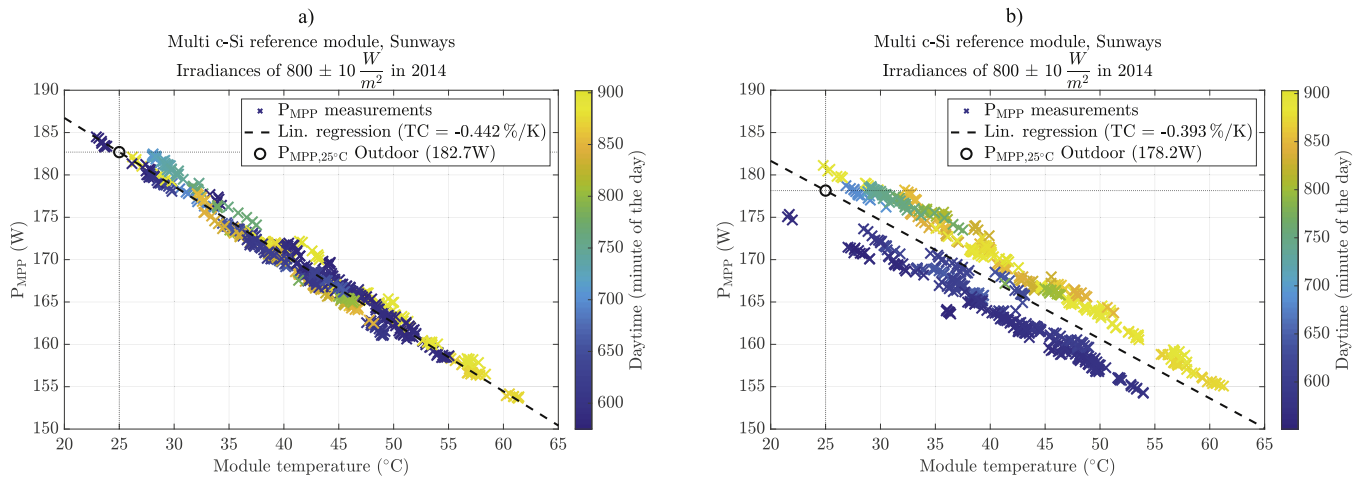


Fig 3 The plots show the MPP power of the multi c-Si reference module with respect to its module temperature over the year 2014. These plots include only data where the irradiance measurements were between 790 W/m^2 and 810 W/m^2 . The analysis in graphic a) is performed by using the non-filtered mono-crystalline silicon ISE reference cell and whereas in the graphic b), the secondary class pyranometer was used. The colouring corresponds to the time of day at which the measurement was performed.

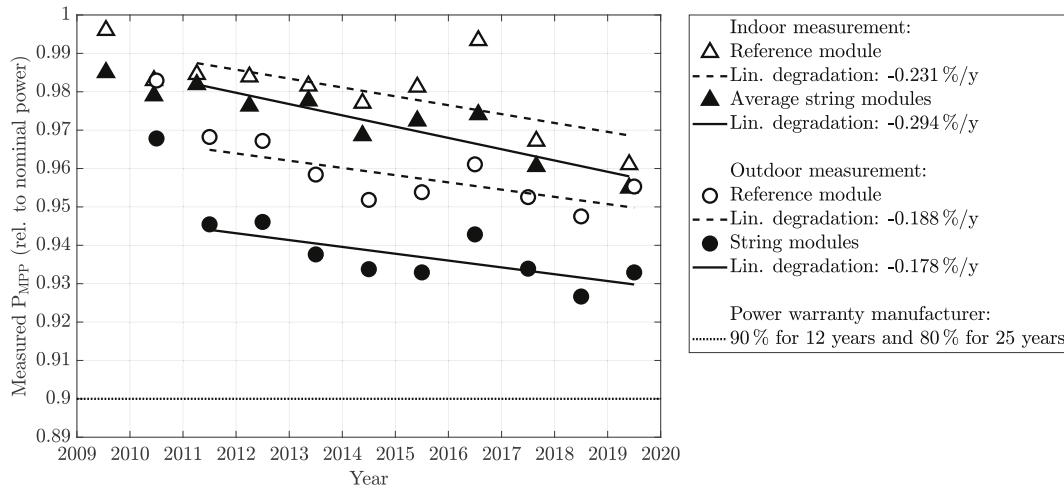


Fig 4 Measured P_{MPP} relative to nominal power of the multi c-Si modules determined by the indoor and outdoor methodology and their corresponding degradation rates

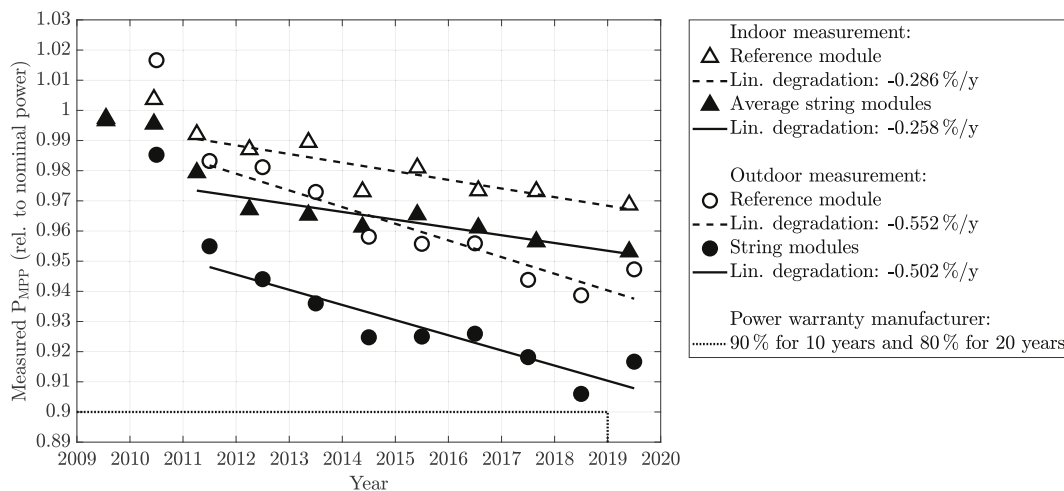


Fig 5 Measured P_{MPP} relative to nominal power of the HIT modules determined by the indoor and outdoor methodology and their corresponding degradation rates

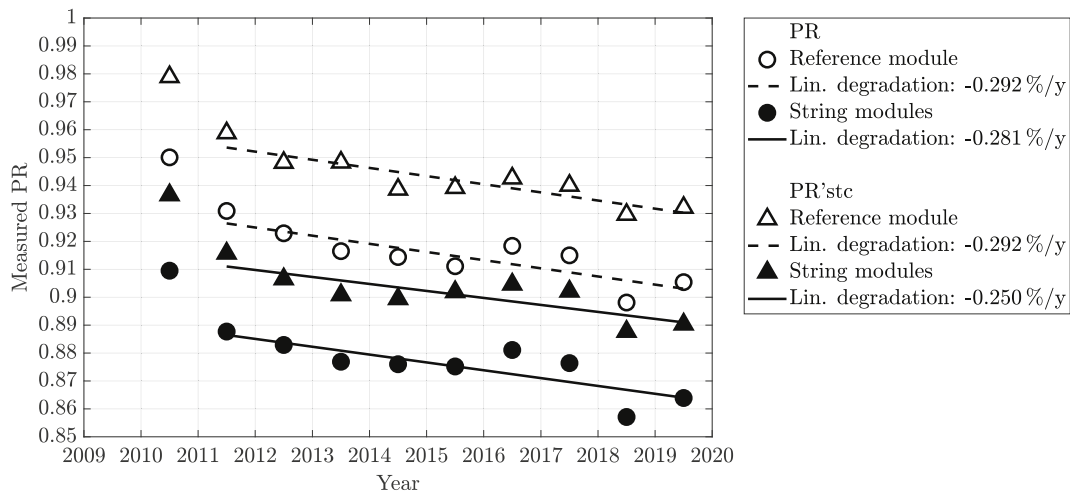


Fig. 6. The resulting degradations within the measured PR of the HIT modules confirm the indoor measurement results

There are much less degradation rate studies available for HIT PV modules than for standard cSi PV modules. The median of the HIT degradation rates was shown to be around 1% for non-continuously monitored PV modules over all climates. The analysed PV module manufactured by Sanyo showed a degradation rate that was smaller by a factor of 2 (outdoor) or 4 (indoor). This shows that the HIT technology does not necessarily have to have much worse ageing. It strongly depends on the individual HIT production technologies and the quality of the PV module manufacturer.

5. Performance ratio comparison between multi cSi and HIT technology

The analysed PR are based on the pyranometer measurements in POA and the initial STC powers of the DUT according to the manufacturer datasheet. In the first year of the comparison, both PV module technologies, cSi and HIT, reveal the same value of PR close to 0.94 (Fig. 7). In addition, the PR_{STC} is calculated according to the standard IEC 61724-1 (2017). At the start of the survey, the PR_{STC} of the cSi PV module is about 2% higher than the corresponding value for HIT due to the higher performance at low irradiance conditions during the whole year. In other words, the benefit of the lower temperature coefficient of the HIT technology is eliminated by its worse low light behaviour. Over the eight years, the spread of about 4% between PR and PR_{STC} does not change for the cSi technology. This is not the case for HIT. In this special

case and after 8 years, the performance losses of the HIT modules due to degradation are in the same range as the losses due to the module temperature.

As expected, the PR of the string is lower than the PR of the single module for both technologies (Fig. 9). However, the lower string performance of the multi cSi modules is driven by the I_{MPP} mismatch and lower string performance of the HIT modules is driven by the increased series resistance and therefore by the lower U_{MPP}.

6. Analysis of temperature coefficient of V_{OC}, V_{MPP} and P_{MPP}

The temperature coefficient of the voltage and power are stable over the 10 years of outdoor operation as expected. Fig. 9 contains the linear regression of V_{OC} and V_{MPP} for 2012. The difference of the temperature coefficient at MPP and open circuit could be quantified and, therefore, a linear relationship of the ratio V_{MPP} to V_{OC} is calculated resulting in value of 0.79 (multi cSi) and 0.82 (HIT) at STC. The corresponding uncertainties are 0.10% and 0.07% at k = 1. These ratios have a temperature coefficient of -0.129%/K for the multi cSi modules and -0.063%/K for the HIT modules as illustrated in Fig. 10. Table 4 compares all measured temperature coefficients by this survey with the temperature coefficient from the manufacturer datasheet. The absolute uncertainties of the temperature coefficient are lower than 0.003%/K (k = 1).

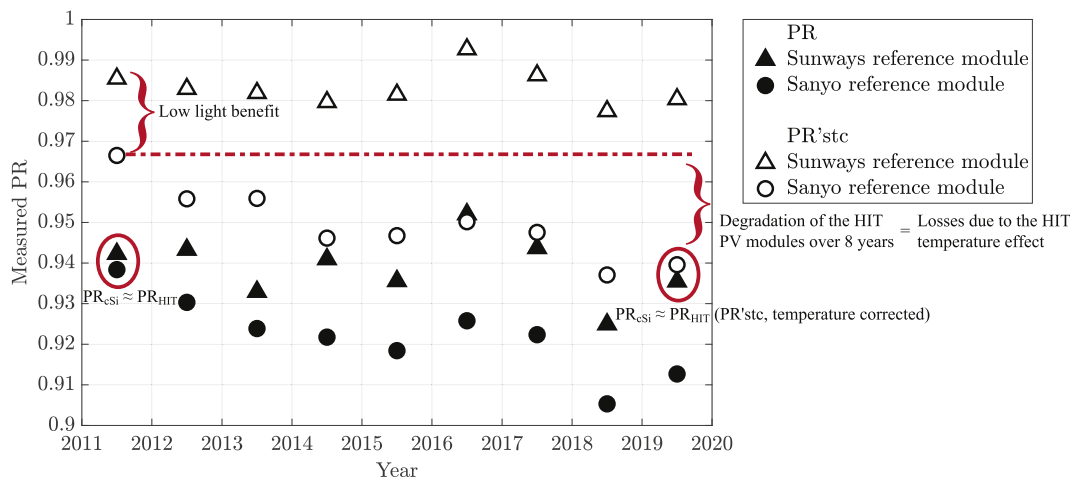


Fig. 7. The PR and PR_{STC} are calculated for the multi cSi and HIT single reference modules

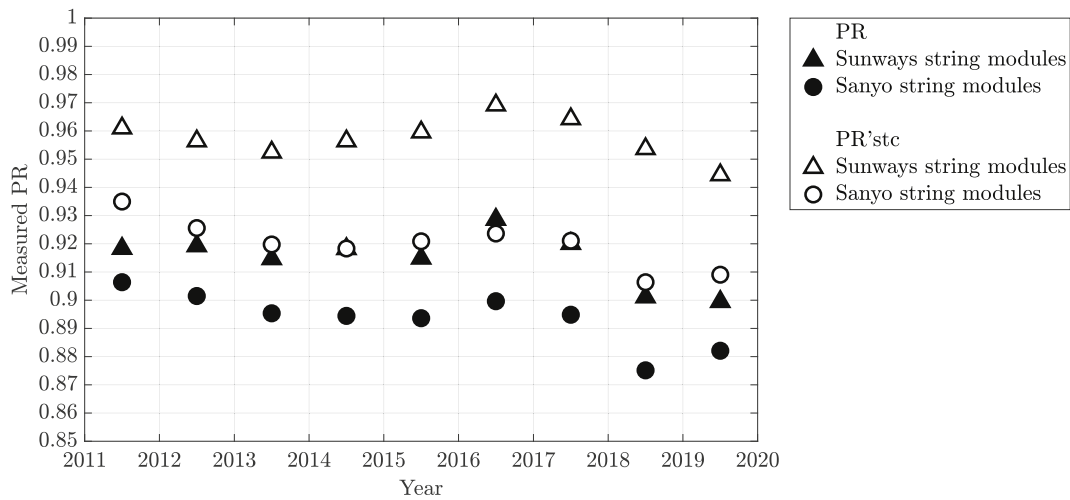


Fig. 8. The PR and PR_{STC} are calculated for the multi oSi and HIT string modules

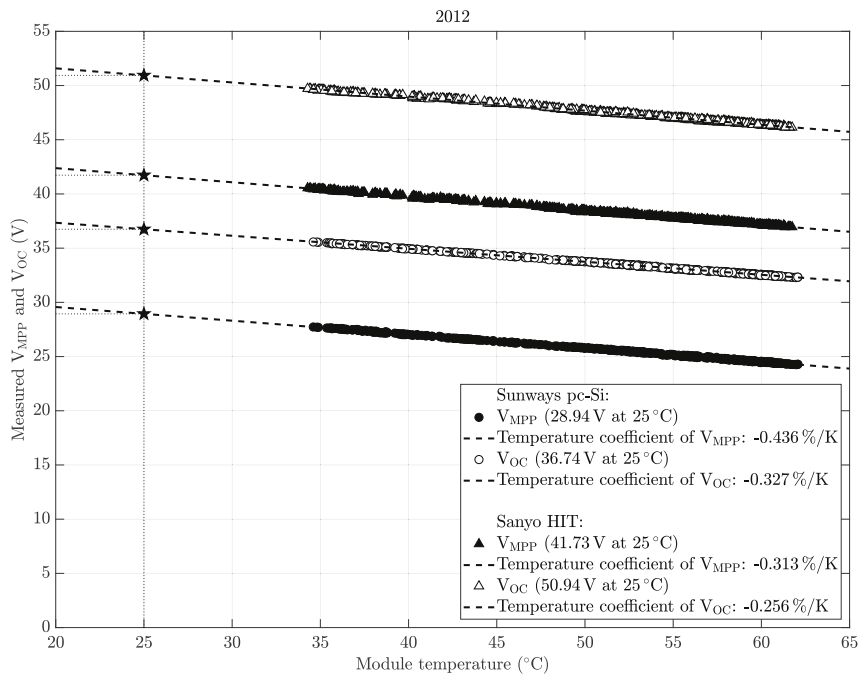


Fig. 9. Linear regression of V_{OC} and V_{MPP} measurements at an irradiance interval of 1000 ± 10W/m² with respect to the module temperature measurements of both module technologies in 2012

7. Conclusion

The annual degradation rates given by the manufacturer are lower than 1.0%. This value is smaller than the uncertainty with which the international test laboratories were able to determine the nominal output than as now. The used method in this work compares identical, unused indoor modules with outdoor modules. In this case, the absolute measurement uncertainty is of less importance than, eg, when comparing energy ratings where the average expanded uncertainty in measurement of P_{MPP} under STC is typically 1.88% [14].

The annual indoor long-term degradation rates of the multi oSi module results are 0.23% ± 0.12% for the single reference module and 0.29% ± 0.08% in average for the string during the survey over nearly the first decade. The annual degradation rates determined from the outdoor measurement are lower, with 0.19% ± 0.07% for the reference module and 0.18% ± 0.08% for the string. This results in a difference of only about 0.6% between both methods over the 8 years, which were

included for the determination of the long-term degradation rates

The analysis of the indoor measurements of the HIT modules shows similar results as the multi oSi modules. The annual degradation is 0.29% ± 0.08% for the single reference module and 0.28% ± 0.08% on average for the string. The outdoor analysis yields annual degradation rates that are twice as high, with 0.58% ± 0.08% and 0.50% ± 0.08%, respectively. The further analysis based on the PR evaluation supports the achieved indoor results for the single and the string modules. The most obvious explanation for these losses is an increased series resistance originating in the cabling system because it appears only at high irradiance in the STC fitting method. The two PV module types have different connectors (Tyco for Sunways and MFC3 for Sanyo modules). The comparison of the outdoor measurements between the multi oSi modules and the HIT modules resulted in a 3.3 times higher voltage drop in the string cabling. However, the single module is measured by four-terminal sensing but that is after the first connector and therefore the connection points are the most obvious source of the losses.

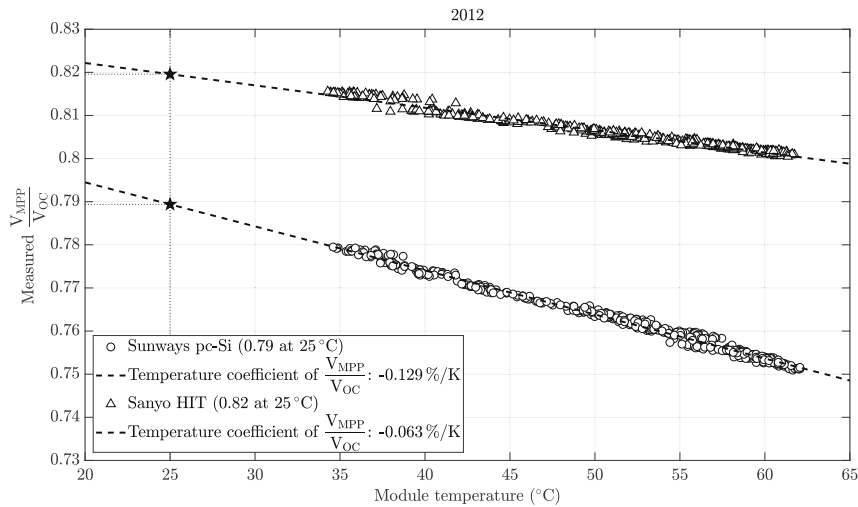


Fig. 10. The ratio of the measured V_{MPP} and V_{OC} behaves linear with respect to the module temperature.

Table 4
Comparison between measured temperature coefficient of V_{OC} , V_{MPP} and P_{MPP} and the corresponding values from the manufacturer datasheet.

| Type | Source | Temperature coefficient (%/K) | | |
|-----------|--------------|-------------------------------|-----------|----------|
| | | P_{MPP} | V_{MPP} | V_{OC} |
| multi cSi | Manufacturer | -0.430 | - | -0.360 |
| | 2012 Module | -0.436 | -0.436 | -0.327 |
| | String | -0.429 | -0.433 | - |
| | 2019 Module | -0.440 | -0.445 | -0.330 |
| HIT | String | -0.428 | -0.430 | - |
| | Manufacturer | -0.300 | - | -0.250 |
| | 2012 Module | -0.318 | -0.313 | -0.256 |
| | String | -0.304 | -0.301 | - |
| | 2019 Module | -0.298 | -0.298 | -0.249 |
| | String | -0.315 | -0.310 | - |

The comparison of the PR with PR_{STC} for both technologies showed that the benefit of the lower temperature coefficient of the HIT technology is eliminated by its worse low light behaviour. In this special case and after 10 years, the performance losses of the HIT modules due to degradation are in the same range as the losses due to the module temperature.

The temperature coefficient of the voltage and power are stable over the 10 years of outdoor operation as expected. The difference of the temperature coefficient at MPP and open circuit could be quantified and, therefore, a linear relationship of the ratio V_{MPP} to V_{OC} is calculated resulting in 0.82 (multi cSi) and 0.79 (HIT) at STC. These ratios have a temperature coefficient of -0.065%/K for the multi cSi modules and -0.128%/K for the HIT modules. These results could help improving the MPP tracking algorithms because of the relationship between V_{MPP} , V_{OC} and module temperature. Further analyses are required regarding other irradiance and shading conditions.

Credit author statement

Fabian Cariget: Methodology, Formal analysis, Investigation, Writing – original draft, Visualization. Franz P. Baumgartner: Conceptualization, Methodology, Validation, Writing – review & editing. Supervision. Christoph J. Brabec: Writing – review & editing. Supervision.

Declaration of competing interest

The authors declare that they have no known competing financial interests or personal relationships that could have appeared to influence the work reported in this paper.

Acknowledgment

We thank Manuel Pezzotti, Jörg Haller, Bruno Aeschbach, Michael Koller, Raphael Knedht, Danilo Grunauer and his team from the electric utility EKZ for their work and support with the infrastructure of the outdoor PV test system and the Swiss Mobile Flasher Bus over the past decade.

We thank the co-author Franz P. Baumgartner that he gave the permission to reuse the photo from Fig. 2d from his publication [7].

References

- [1] Ishii T, Masuda A. Annual degradation rates of recent crystalline silicon photovoltaic modules: annual degradation rates of recent cSi PV modules. *Prog Photovoltaics Res Appl*. Dec. 2017;25(12):953–67. <https://doi.org/10.1002/pip.2903>
- [2] Stein JS, Robinson C, King B, Deline C, Rummel S, Sekulic B. PV lifetime project: measuring PV module performance degradation: 2018 indoor flash testing results. In: 2018 IEEE 7th world conference on photovoltaic energy conversion (WOPEC) (A joint conference of 48th IEEE PVSC, 28th PVSEC & 34th EU PVSEC), waikoloa village, HI; 2018. p. 771–7. <https://doi.org/10.1109/PVSC.2018.8547397>.
- [3] Lopez-Garcia J, Grau-Luque E, Gali S, Kenny RP, Pavanello D, Sample T. Degradation analysis of PV module technologies in a moderate subtropical climate. In: Proceedings of the 36th European photovoltaic solar energy conference and exhibition. Marseille. EUPVSEC; 2019. p. 7. <https://doi.org/10.4229/EUPVSEC20192019-4AV.2.18>
- [4] Jordan DC, Kurtz SR, VanSant K, Newniller J. Compendium of photovoltaic degradation rates. *Prog Photovoltaics Res Appl*. Jul. 2016;24(7):978–89. <https://doi.org/10.1002/pip.2144>
- [5] Allet N, Baumgartner F, Sutterlueti J, Schriener L, Pezzotti M, Haller J. Evaluation of PV system performance of five different PV module technologies. In: Proceedings of the 26th European photovoltaic solar energy conference and exhibition. Hamburg. EUPVSEC; 2011. p. 9. <https://doi.org/10.4229/26thEUPVSEC2011-4DQ.6.2>
- [6] Cariget F, Baumgartner FP, Sutterlueti J, Allet N, Pezzotti M, Haller J. Energy rating based on thermal modelling of five different PV technologies. In: Proceedings of the 29th European photovoltaic solar energy conference and exhibition. Amsterdam. EUPVSEC; 2014. p. 3311–5. <https://doi.org/10.4229/EUPVSEC20142014-5CV.2.34>
- [7] Baumgartner FP, Achtrich T, Allet N, Aeschbach B, Pezzotti M, Koch F, et al. Swiss mobile flasher bus. In: Proceedings of the 24th European photovoltaic solar energy conference and exhibition. Hamburg. EUPVSEC; 2009. <https://doi.org/10.4229/24thEUPVSEC2009-4AV.3.94>
- [8] Achtrich T, Baumgartner FP, Allet N, Pezzotti M, Haller J, Aeschbach B. Swiss mobile flasher bus: progress and new measurement features. In: Proceedings of the 28th European photovoltaic solar energy conference and exhibition. Valencia. EUPVSEC; 2010. <https://doi.org/10.4229/28thEUPVSEC2010-4AV.3.72>
- [9] Baumgartner FP, Schär D, Pezzotti M, Haller J, Polverini D, Tzanelis G, et al. Intercomparison of pulsed solar simulator measurements between the mobile flasher bus and stationary calibration laboratories. In: Proceedings of the 26th European photovoltaic solar energy conference and exhibition. Hamburg. EUPVSEC; 2011. <https://doi.org/10.4229/26thEUPVSEC2011-4AV.1.27>
- [10] Knedht R, Baumgartner F, Cariget F, Frei C, Beglinger F, Zaaman W, et al. Field testing of portable LED flasher non-invasive power measurements of PV modules on-site. In: Proceedings of the 33rd European photovoltaic solar energy conference

- and exhibition. Amsterdam EUPVSEC; 2017. p. 6 <https://doi.org/10.4229/EUPVSEC20172017-600.15.1>.
- [11] Stein JS, Hansen CN, Reno MJ. Global horizontal irradiance clear sky models implementation and analysis. *SAND IWR*. 2012;2012:339.
- [12] Annual degradation multi oSi Trina Solar, Trina solar, [Online]. Available <https://www.trinasolar.com/de/product/duomax72/duomax-psg14> [Accessed 29-May-2020].
- [13] Annual Degradation HIT Panasonic, Panasonic, [Online]. Available <https://euso-lar.panasonic.net/en/2700.html> [Accessed 29-May-2020].
- [14] Blakesley JC, Huld T, Mullejšans H, Gracia-Arillo A, Friesen G, Betts TR, et al. Accuracy, cost and sensitivity analysis of PV energy rating. *Sol Energy Jun. 2020*; 203:91–100 <https://doi.org/10.1016/j.solener.2020.03.088>.